Meteoritics & Planetary Science 37, 1401–1416 (2002)
Available online at http://www.uark.edu/meteor

Properties of chondrules in EL3 chondrites, comparison with EH3 chondrites, and the implications for the formation of enstatite chondrites

D. M. SCHNEIDER[1], S. J. K. SYMES[2], P. H. BENOIT[1]* AND D. W. G. SEARS[1]

[1]Arkansas–Oklahoma Center for Space and Planetary Sciences, Department of Chemistry and Biochemistry, University of Arkansas, Fayetteville, Arkansas 72701, USA
[2]Department of Chemistry, The University of Tennessee at Chattanooga, Chattanooga, Tennessee 37403, USA
*Correspondence author's e-mail address: pbenoit@uark.edu

(Received 2001 July 26; accepted in revised form 2002 June 27)

Abstract–The study of chondrules provides information about processes occurring in the early solar system. In order to ascertain to what extent these processes played a role in determining the properties of the enstatite chondrites, the physical and chemical properties of chondrules from three EL3 chondrites and three EH3 chondrites have been examined by optical, cathodoluminescence (CL), and electron microprobe techniques. Properties examined include size, texture, CL, and composition of both individual phases and bulk chondrules. The textures, distribution of textures, and composition of silicates of the EL3 chondrules resemble those of EH3 chondrules. However, the chondrules from the two classes differ in that (1) the size distribution of the EL chondrules is skewed to larger values than EH chondrules, (2) the enstatite in EL chondrules displays varying shades of red CL due to the presence of fine-grained sulfides and metal in the silicates, and (3) the mesostasis of EH chondrules is enriched in Na relative to that of EL chondrules. The similarities between the chondrules of the two classes suggest similar precursor materials, while the differences suggest that there was not a single reservoir of meteoritic chondrules, but that their origin was fairly local. The differences in the size distribution of chondrules in EH and EL chondrites may be explained by aerodynamic and gravitational sorting during accumulation of the meteoric material, while differences in CL and mesostasis properties may reflect differences in formation conditions and cooling rate following chondrule formation. We argue that our observations are consistent with the formation of enstatite chondrites in a thick dynamic regolith on their parent body.

INTRODUCTION

The chondrules in ordinary and carbonaceous chondrites have been well studied, and textures, bulk compositions, and mineral compositions have been used to classify chondrules as an aid to interpreting their formational histories (*e.g.*, McSween, 1977a,b; King and King, 1978, 1979; Dodd, 1981; Gooding and Keil, 1981; Scott and Taylor, 1983; Rubin and Keil, 1984; Rubin, 1989; Sears *et al.*, 1992; Jones, 1994; Huang *et al.*, 1996). Dodd (1981) argued that while chondrules in ordinary chondrites were mainly "lithic", or porphorytic, types, chondrules in carbonaceous chondrites were predominantly "droplet", or glass-rich or fine-grained, types, and that the different classes had fundamentally different histories. Later classification schemes focused on mineral composition and bulk composition, such as the separation into type I (with FeO-poor olivines) and type II (with FeO-rich olivines) chondrules (McSween, 1977a), subdivided by calcium abundance in olivine (Scott and Taylor, 1983; Jones 1990, 1994). Another classification system for ordinary and carbonaceous chondrules focused on olivine and mesostasis composition (Sears *et al.*, 1992; DeHart *et al.*, 1992; Huang *et al.*, 1996). The placement of chondrules from enstatite chondrites in these systems has not been extensively explored. In this paper, we focus on chondrules from the least metamorphosed EL chondrites, documenting basic chondrule properties, comparing these data to chondrules from EH chondrites, and seek to interpret these data in terms of possible chondrule formation mechanisms suggested for chondrules from the major meteorite groups.

Previous work on chondrules from enstatite chondrites was concentrated on EH chondrites. These include an investigation of over 100 individual chondrules isolated from the Indarch (EH4) enstatite chondrite by Leitch and Smith (1982), Leitch *et al.* (1982), and Smith *et al.* (1983). Rambaldi *et al.* (1983) and Grossman *et al.* (1985) examined relic grains, or precursor components, in the chondrules of Qingzhen, a highly unequilibrated EH3 chondrite. Ikeda (1988, 1989) conducted

Prelude preprint MS#4610

an intensive petrochemical study of over 100 chondrules in thin sections from the EH3 chondrite Yamato (Y)-691.

The scarcity of work on chondrules from EL chondrites has reflected the lack of suitable samples, as virtually all EL chondrites are equilibrated, and thus contain few identifiable chondrules. Only a few unequilbrated EL chondrites are known, all recently discovered finds (Grossman and Score, 1996). In this study, we examine three Antarctic meteorites, Allan Hills (ALH) 85119, MacAlpine Hills (MAC) 88180 and Pecora Escarpment (PCA) 91020.

EXPERIMENTAL METHODS

Three EL3 chondrite thin sections (ALH 85119,11; MAC 88180,14; and PCA 91020,16), and three EH3 chondrite thin sections (ALH 84170,15; PCA 91085,7; and PCA 91238,8), were examined in this study. Chondrule sizes, textures, and CL characteristics of all chondrules were recorded and mineral, mesostasis, and bulk chondrule compositions were determined in representative chondrules from the EL3 sections and from the PCA 91238 section.

All chondrules were assigned a Gooding and Keil (1981) textural description. Textural categories assigned include porphyritic pyroxene (PP), radial pyroxene (RP), porphyritic olivine-pyroxene (POP), granular (G), and cryptocrystalline (C). The average size and the size distribution of the chondrules were determined following the procedures of King and King (1978, 1979). The data analysis procedures of Eisenhour (1996) were not used, due to the small number of chondrules in this study. Chondrule fragments apparently exhibiting <180° of coverage were excluded. The diameters of 199 chondrules from the three EL3 sections and 135 chondrules from the three EH3 sections were determined. Cathodoluminescence mosaics were prepared from the thin sections using a commercial Nuclide Instruments "Luminoscope" operated at 13 ± 1 kV and 0.8 ± 0.1 mA, which was attached to a low-magnification optical microscope.

Major and minor element compositional data were determined for 27 EL3 chondrules (eight in ALH 85119, nine in MAC 88180 and ten in PCA 91020) and four EH3 chondrules (in PCA 91238) using the Cameca SX100 electron microprobe at Johnson Space Center (JSC). Silicate phases (low and high Ca pyroxene, olivine and a nearly pure SiO_2 phase) were analyzed using a focused (~1 μm diameter) beam in point mode, 15 kV accelerating voltage, and 20 nA gun current. Five to 15 spots per grain were analyzed and the data averaged. Mesostasis analyses were complicated by the presence of microcrystallites, therefore mesostasis compositional data were obtained by rastering the electron beam over a 6 μm square. Chondrule bulk compositions were determined by rastering a focused electron beam over thirty to fifty 30 μm squares and averaging the counts. Natural mineral standards were used for calibration and the data were reduced by the PAP matrix correction program. Repeated analyses of mineral standards indicate reproducibility of measurement for all elements to within 2%.

RESULTS

The chondrules in EL3 chondrites display a range of textures similar to those seen in the ordinary chondrites (Gooding and Keil, 1981) and in EH3 chondrites (Grossman *et al.*, 1985; Ikeda, 1989). The PP chondrules are most abundant, with RP, POP, and G chondrules occurring less frequently, and C chondrules being relatively rare (Table 1; Fig. 1).

The chondrules in the two classes of meteorites have different average sizes. Table 2 gives the average diameter, and Fig. 2 shows the frequency histograms. The chondrules in the EH3 chondrites have an average diameter of 278 ± 229 μm (1σ) and a range of 45–1313 μm, and the EL3 chondrules have an average diameter of 476 ± 357 μm (1σ) and a range of 85–2125 μm. The size distribution of chondrules in EL3 chondrites is approximately log normal, while the size distribution of EH3 chondrules is skewed to larger sizes. This trend in EH chondrules was also noted by Rubin and Grossman (1987) in

TABLE 1. Distribution of textures in enstatite chondrites.

Meteorite(s)	Number of chondrules					
	PP	POP	RP	G	C	Total
Allan Hills 85199 (EL3)	15	9	4	6	1	35
MacAlpine Hills 88180 (EL3)	21	8	4	2	3	38
Pecora Escarpment 91020 (EL3)	81	18	13	13	1	126
Allan Hills 84170 (EH3)	20	11	2	6	1	40
Pecora Escarpment 91085 (EH3)	22	0	5	9	8	44
Pecora Escarpment 91238 (EH3)	35	5	2	10	0	52
Qingzhen, Kota-Kota, Allan Hills 77156 (EH3)*	535	32	90	10	35	702

Abbreviations: PP = porphyritic pyroxene; POP = porphyritic olivine-pyroxene; RP = radial pyroxene; G = granular; C = cryptocrystalline.
*From Rubin and Grossman (1987).

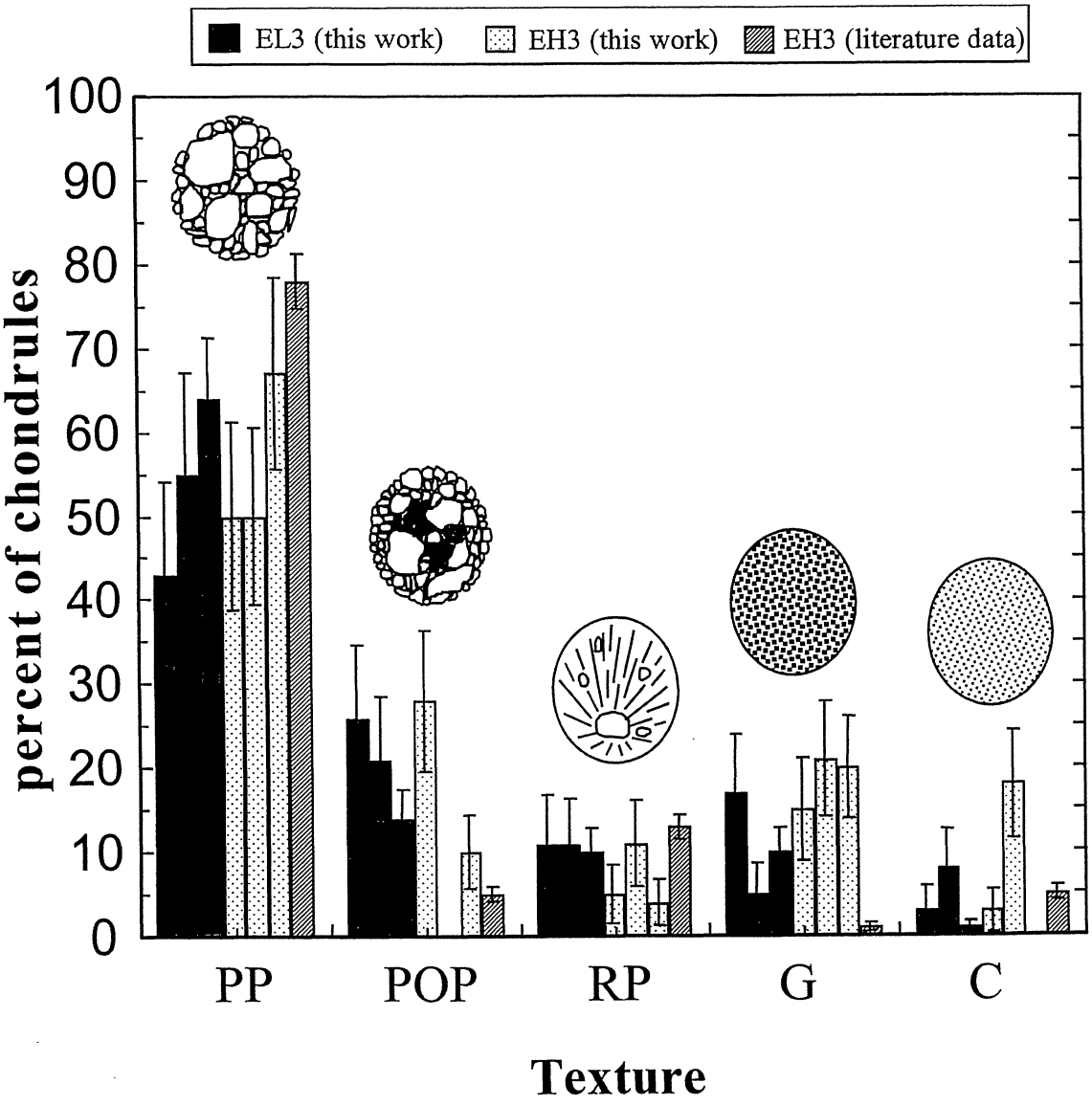

FIG. 1. Chondrule textures in enstatite chondrites. The meteorites studied include three EL3 chondrites (ALH 85119, MAC 88180, and PCA 91020, respectively) and three EH3 chondrites (ALH 84170, PCA 91085, and PCA 91238, respectively). Literature data for the EH3 chondrites Qingzhen, Kota-Kota, and ALHA77156 is also shown (Grossman *et al.*, 1985; Rubin and Grossman, 1987). Texture designations are from Gooding and Keil (1981) (see text for meanings of texture abbreviations). The distribution of textures is similar for both classes, indicating a common range of formation conditions for the chondrules. Error bars reflect uncertainties estimated from total number of chondrules in each database.

chondrules from Qingzhen, Kota Kota, and ALHA77156, and was attributed to the inadvertent exclusion of small chondrules.

Rubin and Grossman (1987) suggested that while both porphyritic and nonporphyritic chondrules of EH chondrites have approximately log-normal size distributions, the nonporphyritic chondrules have a broader distribution, so that the nonporphyritic chondrules dominate at both ends of the size spectrum. We observed that the sizes of porphyritic and nonporphyritic chondrules vary between the two classes and that the porphyritic chondrules in EH chondrites are somewhat larger than the nonporphyritic chondrules, and have an approximately log-normal distribution. On the other hand, the nonporphyritic chondrules tend to have a distribution skewed toward only larger sizes (Fig. 3). Chondrules of the EL3 chondrites do not show these trends, instead having similar average sizes and relatively log-normal distributions in both porphyritic and nonporphyritic chondrules. The nonporphyritic chondrule distribution appears skewed, but this may be a measurement artifact from the smallest chondrules.

TABLE 2. Chondrule sizes and aspect ratios for all measured chondrules.

No.	avg. diam. (μm)	asp. ratio
ALH 85119		
1	1875	1.38
2	300	1.18
3	235	1.04
4	1840	1.54
5	435	1.23
6	670	1.31
7	420	1.21
8	200	1.11
9	130	1.00
10	570	1.24
11	690	1.38
12	390	1.44
13	420	1.40
14	115	1.30
15	440	1.51
16	295	1.19
17	285	1.28
18	395	1.19
19	360	1.18
20	990	1.08
21	315	1.42
22	440	1.26
23	220	1.20
24	470	1.19
25	285	1.28
26	235	1.35
27	265	1.41
28	405	1.45
29	660	1.13
30	1128	1.58
31	560	1.49
32	255	1.43
33	660	1.32
34	370	1.11
35	285	1.28
MAC 88180		
1	2125	1.00
2	225	0.96
3	85	1.13
4	400	1.16
5	175	1.19
6	320	1.00
7	330	1.28
8	425	1.18
9	220	1.59
10	505	1.02
11	650	1.32
12	295	1.57
13	635	1.23
14	160	1.13
15	620	1.25
16	225	1.25
17	155	1.21
18	715	1.27
19	375	1.27
20	280	1.00
21	245	0.96
22	530	1.00
23	490	1.13
24	290	1.32
25	345	1.38
26	430	1.53
27	605	2.18
28	355	1.29
29	565	1.40
30	838	1.68
31	475	1.11
32	765	1.55
33	250	1.38
34	365	0.92
35	290	1.23
36	350	1.41
37	1025	1.00
38	605	1.33
PCA 91020		
1	1488	1.20
2	260	1.17
3	235	1.35
4	450	1.43
5	590	1.19
6	195	1.44
7	850	1.00
8	380	1.05
9	690	1.51
10	330	1.64
11	450	1.14
12	915	1.26
13	420	1.33
14	225	1.25
15	1225	1.33
16	365	1.61
17	255	1.22
18	270	1.35
19	500	1.50
20	330	1.28
21	1250	1.50
22	1050	1.15
23	450	1.50
24	510	1.68
25	590	1.31
26	440	1.00
27	260	1.48
28	475	1.79
29	600	1.31
30	480	1.53
31	315	1.52
32	585	1.25
33	335	1.31
34	740	1.55
35	505	1.10
36	460	1.04
37	285	1.04
38	850	1.62
39	613	2.06
40	705	1.43
41	455	1.68
42	315	2.00
43	585	1.39
44	1175	2.76
45	1638	1.34
46	315	1.25
47	310	1.14
48	425	2.15
49	355	1.29
50	470	1.47
51	510	1.76
52	350	1.59
53	220	1.32
54	305	1.10
55	250	1.38
56	1075	1.05
57	410	1.10
58	285	1.38
59	515	1.45
60	280	1.00
61	470	1.35
62	630	1.33
63	140	1.55
64	220	1.00
65	180	1.12
66	270	2.18
67	290	1.52
68	185	1.31
69	430	1.39
70	170	1.43
71	425	1.43
72	320	2.20
73	245	1.13
74	145	1.23
75	165	1.36
76	355	1.15
77	645	1.48
78	150	1.31
79	90	1.25
80	1188	1.50
81	290	1.64
82	320	1.37
83	215	2.07
84	225	1.37
85	150	1.31
86	185	1.18
87	100	1.22
88	250	1.50
89	470	1.69
90	215	1.53
91	200	1.67
92	655	1.11
93	475	1.44
94	335	1.39
95	560	1.55
96	240	1.53
97	265	1.12
98	310	1.48
99	1263	1.53
100	415	1.52
101	225	1.14
102	375	1.78
103	620	1.38
104	280	1.43
105	320	1.37
106	355	1.45
107	1950	1.00
108	205	1.16
109	315	1.25
110	280	1.33
111	750	1.38
112	305	1.26
113	1200	1.23
114	510	1.68
115	395	1.32
116	235	1.61
117	215	1.53
118	150	1.14
119	330	1.44
120	370	1.00
121	455	1.53
122	370	1.00
123	320	1.78
124	405	1.70
125	240	1.67
126	640	1.25
ALH 84170		
1	1038	1.24
2	413	1.06
3	475	1.24
4	538	1.26
5	500	1.11
6	238	1.11
7	110	1.00
8	275	1.44
9	1213	1.20
10	160	1.13
11	538	1.39
12	375	1.14
13	425	1.43
14	300	1.07
15	125	1.08
16	190	1.38
17	155	1.21
18	235	1.24
19	195	1.79
20	190	1.11
21	160	1.00
22	275	1.50
23	200	1.11
24	413	1.06
25	650	1.17
26	95	1.11
27	215	1.15
28	250	1.17
29	95	1.11
30	220	1.10
31	160	1.13
32	305	1.10
33	210	1.47
34	100	1.22
35	165	1.20
37	195	1.05
38	70	1.00
39	170	1.13
40	600	1.29
41	550	1.00
PCA 91085		
1	545	1.14
2	120	1.00
3	200	1.00
4	50	1.00
5	250	1.50
7	230	1.00
8	355	1.15
9	90	1.25
10	880	1.05
11	115	1.09
12	80	1.00
13	120	1.18
14	315	1.25
15	90	1.00
16	345	1.16
17	100	1.00
18	1000	1.11
19	230	1.30
20	145	1.07
21	300	1.07
22	80	1.29
23	95	1.11
24	675	1.25
25	90	1.25
26	195	1.05
27	205	1.41
28	255	1.32
29	180	1.12
30	140	1.15
31	95	1.11
32	370	1.31
33	190	1.11
34	95	1.11
35	100	1.22
36	135	1.25
37	65	1.17
38	130	1.00
39	155	1.07
40	515	1.24
41	120	1.18
42	390	1.05
43	110	1.00
44	205	1.16
45	495	1.25
PCA 91238		
1	900	1.00
2	688	1.20
3	375	1.31
4	763	1.35
5	425	1.07
6	320	1.21
7	385	1.20
8	240	1.18
9	295	1.03
11	385	1.03
12	320	1.00
13	200	1.11
14	600	1.26
15	220	1.10
16	190	1.53
17	170	1.13
18	160	1.29
19	115	1.30
20	185	1.31
21	210	1.10
22	140	1.33
23	90	1.00
24	115	1.09
25	125	1.27
26	180	1.25
27	85	1.13
28	220	1.59
29	190	1.53
30	105	1.10
31	185	1.06
32	170	1.27
33	570	1.59
34	395	3.94
35	220	1.20
36	60	1.00
37	105	1.10
38	590	1.95
39	165	1.36
40	170	1.13
41	120	1.00
42	145	1.07
43	90	1.00
44	200	1.00
45	460	1.30
46	335	1.31
47	175	1.19
48	120	1.18
49	140	1.33
50	45	1.25
51	250	1.50
52	105	1.10

Abbreviations: No. = chondrule number, arbitrarily designated; ALH = Allan Hills; MAC = MacAlpine Hills; PCA = Pecora Escarpment; avg. = average; diam = diameter; asp. = aspect.

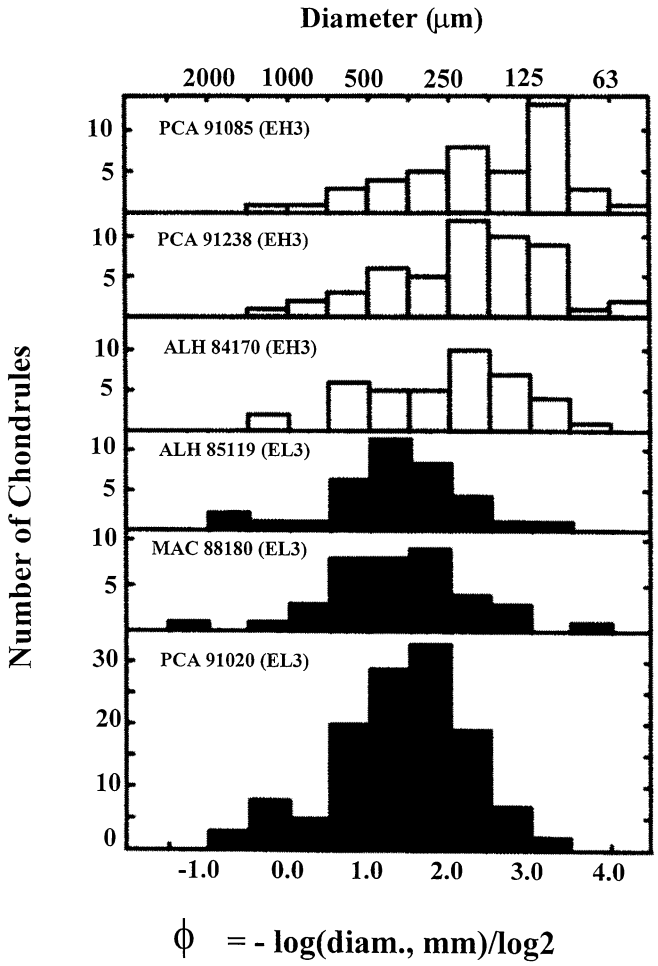

FIG. 2. Size distribution of chondrules in EH and EL chondrites. Although the range of sizes is similar between the two classes, the average chondrule size tends to be larger in the EL chondrites (476 ± 357 μm, mean and 1σ) as compared to the EH chondrites (278 ± 229 μm). There is also a tendency for the chondrules in EH chondrites to be skewed toward larger sizes, while the chondrules in the EL chondrites have a more log-normal distribution.

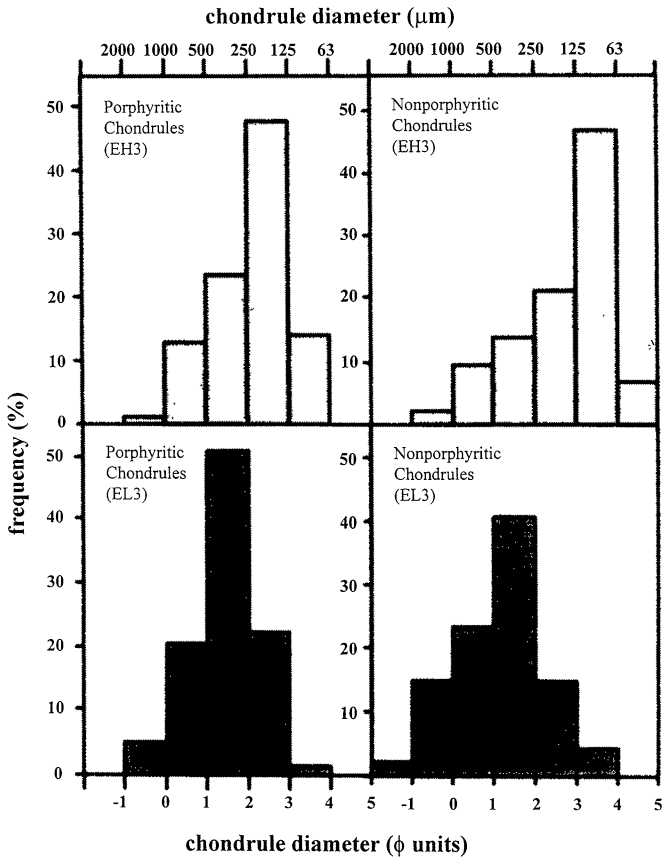

FIG. 3. Sizes of porphyritic (PP and POP) *vs.* nonporpyhritic (RP, G, and C) chondrules for all enstatite chondrites measured in this work. While porphyritic chondrules in EH3 chondrites tend to be larger with a relatively log-normal distribution, nonporphyritic chondrules have a smaller average size with a distribution skewed to larger sizes. Similar trends were noticed in EH chondrites by Rubin and Grossman (1987), except that they found nonporphyritic chondrules dominated the small size fraction as well. Chondrules in EL3 chondrites do not show this same trend, instead having similar average sizes and relatively log-normal distributions for both porphyritic and nonporphyritic chondrules. This may be reflecting differences in the formation events of the nonporphyritic chondrules in the two classes, or it may indicate different sorting mechanisms for the chondrules in EH and EL chondrites.

The chondrules of both EL and EH chondrites are relatively spherical, although the chondrules in EH3, and more so in EL3 chondrites, are somewhat "flattened", with average aspect ratios of 1.21 ± 0.29 and 1.36 ± 0.26, respectively (Table 2; Fig. 4). There is some alignment of chondrule flattening in each EL3 chondrite section (Fig. 5). Rubin *et al.* (1997) have made the same observation of EL3 chondrites, and since EL3 chondrites have shock stages of S2 or S3 (Rubin *et al.*, 1997), this led them to attribute the foliation to impact deformation by a mechanism similar to those suggested by Scott *et al.* (1992) and Nakamura *et al.* (1992, 1995) in which flattened chondrules were squeezed into matrix pores that collapsed at shock pressures of greater than 5–10 GPa.

The chondrules in the EL3 chondrites are composed primarily of enstatite with a mixture of red cathodoluminescence (CL) of various intensities, and occasionally blue CL. Figure 5 shows a sketch of the CL colors of the various components observed in EL3 chondrites. The enstatite with lighter red CL is the most common, and proved difficult to analyze in all chondrules examined because of numerous micron and sub-micron sized inclusions (Fig. 6). It was noted that the majority of POP chondrules (inset, Fig. 5) have an intense dark red CL with inclusions of olivine displaying a yellow-orange CL. The PP, RP, and C chondrules range from dark to light red in CL color, with inclusions of bright blue glass or dull blue to black mesostasis.

Chondrules in EH3 chondrites exhibit the same CL properties as chondrules in EL3 chondrites, except for having

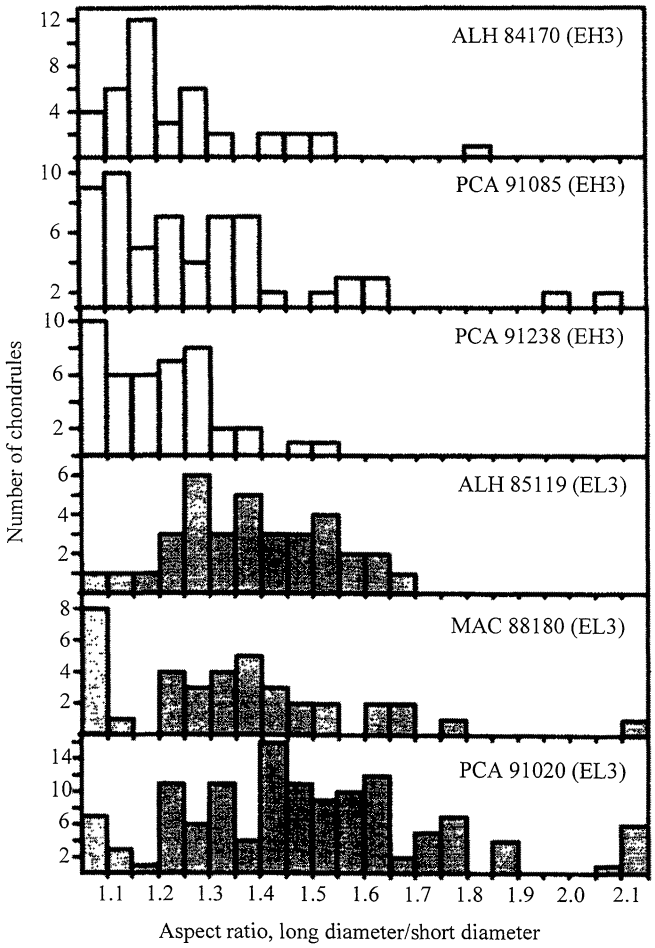

FIG. 4. Aspect ratios of chondrules in EH3 and EL3 chondrites. Chondrules in EL3 chondrites tend to be less spherical (average ratio 1.36 ± 0.26) than their EH3 counterparts (average ratio 1.21 ± 0.29). The direction of elongation of the chondrules is along the same axis within the meteorites (see Fig. 5). This trend was also observed by Rubin *et al.* (1997) in many of the enstatite chondrites, and was attributed to impact deformation.

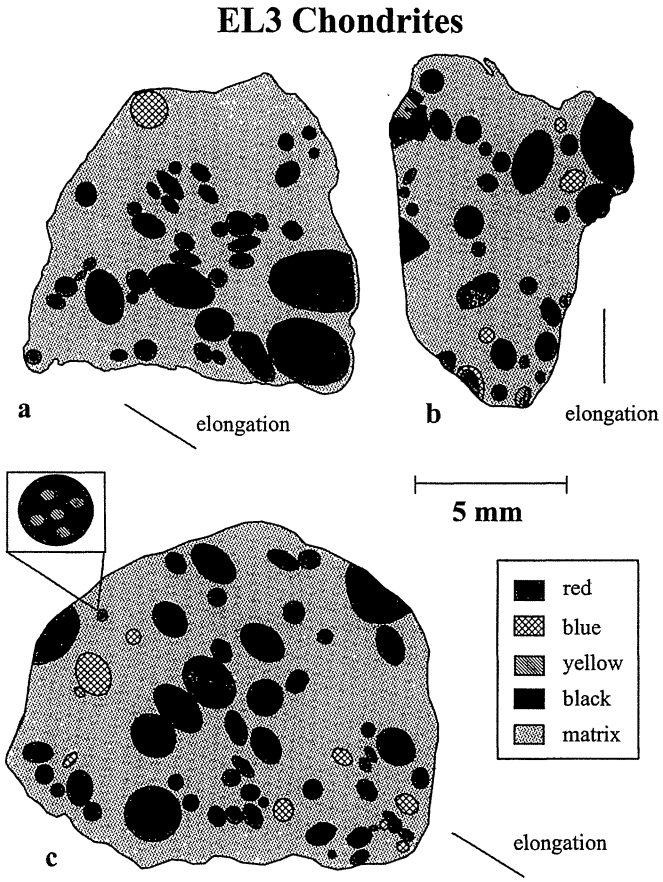

FIG. 5. Cathodoluminescence "maps" of EL3 chondrite thin sections. (a) ALH 85119,11; (b) MAC 88180,14; (c) PCA 91020,16. Outlines of all chondrules and some clasts are shown for each section. A preferred direction of elongation of the chondrules is given for each section. The inset in (c) illustrates a POP chondrule with yellow luminescing olivine and red luminescing pyroxene. Red luminescing material of various shades and intensities by far dominates the material in the EL3 chondrites and appears to be evenly distributed throughout the meteorite; EH3 chondrites, not shown here, have a more even distribution of red and blue luminescing material.

a lighter red luminescence that is rare in the EH3 chondrules. These observations are consistent with those of Weisberg *et al.* (1994) who noted that many chondrules in unequilibrated enstatite chondrites display certain CL that reflect their mineralogy. Most commonly they found red and blue enstatites occurring in chondrules, but they also found some chondrules containing FeO-rich pyroxene with no CL, which they termed "black" CL, that are rimmed by minor element-poor rims with blue CL. These non-luminescent pyroxenes would often contain areas of FeO-poor enstatite with red CL, associated with millimeter-sized blebs of metal and sometimes silica. Weisberg *et al.* interpreted these grains as resulting from reduction of initially more oxidized material subsequent to agglomeration of the meteorite.

The minor element composition of the pyroxene and olivine in the chondrules from EL3 chondrites are very similar to those of chondrules from EH3 chondrites reported both here and in the literature (Table 3; Fig. 7). Silicate compositions vary from chondrule to chondrule and even between grains within individual chondrules, and although not shown here, we found no relationship between composition and CL or composition and texture that would distinguish the two classes. However, the composition of the mesostasis in chondrules from EH and EL chondrites varies significantly (Table 3; Fig. 8), with the chondrules of EL chondrites being poor in sodium (0–4 wt% Na_2O) relative to those in EH chondrites (~9 wt% Na_2O) (Table 3). Grossman *et al.* (1985) also found a high sodium content in the mesostasis of chondrules in EH chondrites (7–12 wt% Na_2O).

In order to determine if the sodium difference in the mesostasis of the chondrules is due to diffusion of the sodium from the mesostasis to the surrounding silicates, we determined

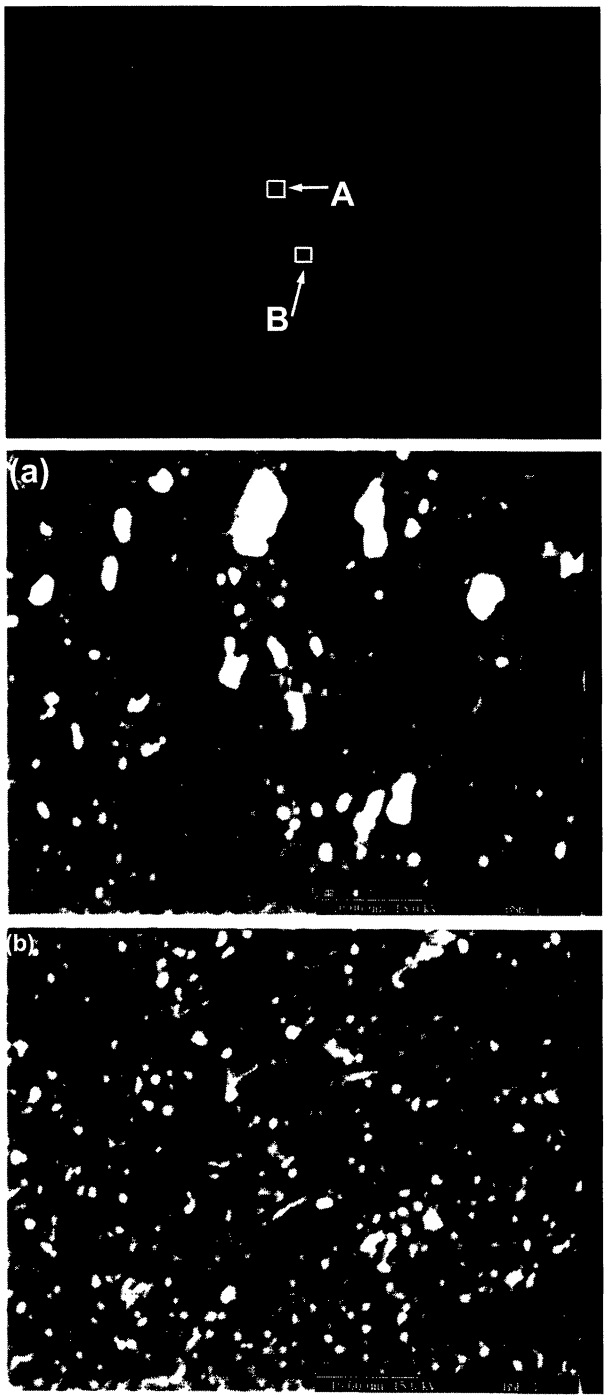

FIG. 6. "Dusty" enstatite in chondrules. The top image is a black and white cathodoluminescence image of chondrule 1 in PCA 91020 (field of view is ~2 mm). (a) BSE image of a darker red area of the chondrule (field of view, 50 μm) shows fewer but larger grains of metal concentrated in the spaces between grains. (b) BSE image of a brighter red area of the chondrule (field of view, 50 μm) showing a higher abundance of small metal grains uniformly distributed within the silicates. These images are typical for the light to dark red areas of enstatite within the chondrules, and is likely attributed to either liquid immiscibility between silicate and metal–sulfide melts or to *in situ* reduction of FeO from olivine.

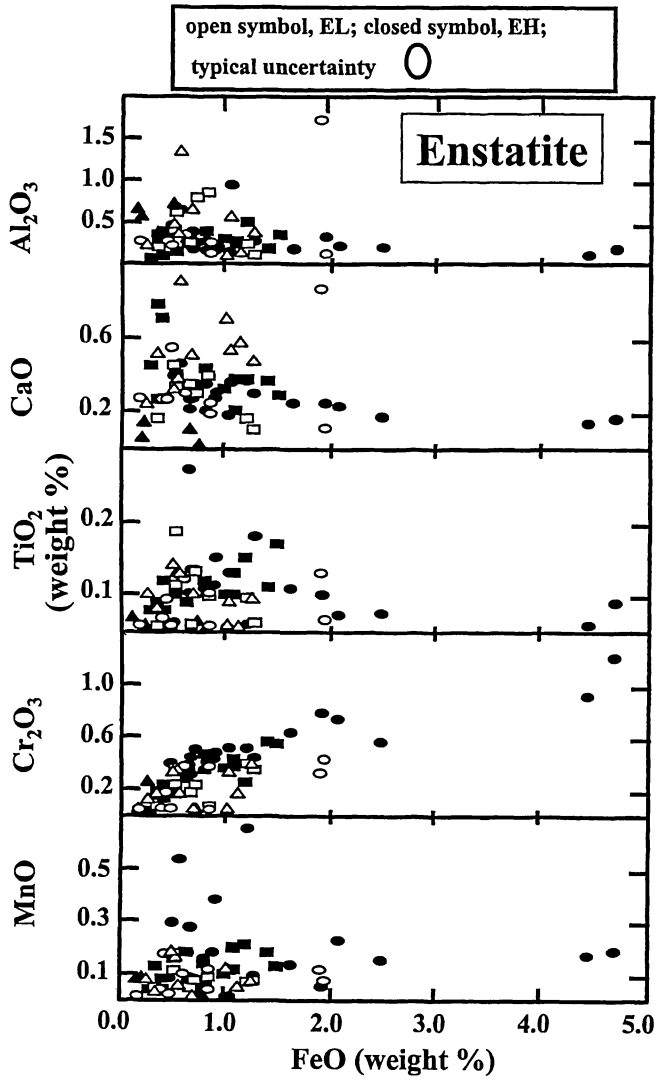

FIG. 7. Minor element compositions of enstatite in EH and EL chondrite chondrules. For the EL chondrites (open symbols), squares indicate ALH 85119, circles indicate MAC 88180, and triangles indicate PCA 91020 (all this work); for EH chondrites (filled symbols), squares indicate Qingzhen (Grossman *et al.*, 1985), circles indicate Y-691 (Ikeda, 1988, 1989), and triangles indicate PCA 91238 (this work). Also shown is the size of the typical analytical uncertainty. The minor element compositions of enstatite in EH and EL chondrites are very similar; although not plotted here, we also found no correlation between texture and composition or CL and composition of the chondrules between the two classes. This would indicate similar formation conditions for the chondrules of both classes.

the bulk composition of several chondrules with notable amounts of mesostasis (Table 4). EL3 chondrules show slight enrichments in TiO_2 and CaO, while Na_2O is slightly lower. Na_2O and Al_2O_3 show a correlation in which the ratio is 0.26 for EL chondrules and 0.50 for EH chondrules (Fig. 9). The small differences between EH and EL chondrules in bulk composition (Table 4) reflects the small amount of mesostasis present in the chondrules.

TABLE 3. Composition (wt%) of pyroxene, olivine, and mesostasis in EH3 and EL3 chondrules.

#	Phase	Pts.	SiO_2	Al_2O_3	Cr_2O_3	FeO	MnO	MgO	CaO	Na_2O	TiO_2	Total*
Allan Hills 85119: EL3												
2	Pyrox	3	59.9 ± 0.7	0.9 ± 0.7	0.07 ± 0.05	0.9 ± 0.4	0.09 ± 0.05	38 ± 2	0.4 ± 0.3	b.d.	0.05 ± 0.05	100.6
3	Pyrox	14	59.9 ± 0.3	0.21 ± 0.05	0.1 ± 0.1	0.4 ± 0.3	0.05 ± 0.07	39.6 ± 0.3	0.17 ± 0.05	b.d.	b.d.	100.4
6	Pyrox	8	59.7 ± 0.2	0.11 ± 0.02	0.35 ± 0.03	1.3 ± 0.4	0.08 ± 0.02	39.2 ± 0.4	0.11 ± 0.02	b.d.	b.d.	100.9
7	Pyrox	6	59.3 ± 0.8	0.4 ± 0.2	0.2 ± 0.1	0.5 ± 0.1	0.18 ± 0.08	39.0 ± 0.5	0.45 ± 0.08	b.d.	0.06 ± 0.04	100.2
12	Pyrox	10	58.9 ± 0.8	0.8 ± 0.7	0.2 ± 0.2	0.7 ± 0.2	0.08 ± 0.04	38.9 ± 0.5	0.30 ± 0.09	b.d.	0.08 ± 0.03	100.2
21	Pyrox	14	59.6 ± 0.7	0.3 ± 0.1	0.2 ± 0.2	0.7 ± 0.6	0.05 ± 0.06	39.3 ± 0.5	0.4 ± 0.3	b.d.	b.d.	100.5
34	Pyrox	4	59.1 ± 0.5	0.24 ± 0.03	0.40 ± 0.03	1.2 ± 0.2	0.07 ± 0.02	39.0 ± 0.4	0.17 ± 0.03	b.d.	0.05 ± 0.01	100.3
37	Pyrox	5	59.4 ± 0.1	0.62 ± 0.08	0.62 ± 0.08	0.37 ± 0.03	0.11 ± 0.02	39.2 ± 0.4	0.34 ± 0.04	b.d.	0.14 ± 0.01	100.7
11	Oliv	2	42.9 ± 0.1	0.08 ± 0.05	0.18 ± 0.07	0.38 ± 0.09	0.14 ± 0.02	56.6 ± 0.6	0.22 ± 0.03	b.d.	b.d.	100.5
37	Meso.	10	60 ± 2	21 ± 1	0.06 ± 0.02	2.2 ± 0.9	b.d.	6 ± 3	3.6 ± 0.5	2 ± 1	0.4 ± 0.1	94.6
MacAlpine Hills 88180: EL3												
1	Pyrox	5	60.4 ± 0.2	0.3 ± 0.3	b.d.	0.2 ± 0.05	b.d	40.3 ± 0.2	0.28 ± 0.07	b.d.	b.d.	101.4
3	Pyrox	14	59.6 ± 0.5	0.37 ± 0.07	0.37 ± 0.03	0.62 ± 0.05	0.1 ± 0.01	39.5 ± 0.3	0.31 ± 0.03	b.d.	0.07 ± 0.01	100.9
11	Pyrox	8	55 ± 1	0.7 ± 0.4	0.2 ± 0.2	7 ± 2	0.08 ± 0.06	35 ± 2	2 ± 2	0.07 ± 0.09	0.07 ± 0.06	100.2
12	Pyrox	5	59.4 ± 0.1	0.6 ± 0.2	0.43 ± 0.04	0.73 ± 0.4	0.08 ± 0.03	39.1 ± 0.2	0.5 ± 0.4	b.d.	0.09 ± 0.03	100.9
16	Pyrox	5	59.5 ± 0.6	0.13 ± 0.04	0.44 ± 0.02	1.94 ± 0.06	0.07 ± 0.01	38.5 ± 0.4	0.12 ± 0.03	b.d.	b.d.	100.7
24	Pyrox	12	60.2 ± 0.4	0.2 ± 0.1	b.d.	0.5 ± 0.3	b.d.	40.3 ± 0.3	0.6 ± 0.3	b.d.	b.d.	101.9
25	Pyrox	6	60 ± 2	2 ± 2	0.3 ± 0.2	1.9 ± 0.8	0.12 ± 0.04	35 ± 3	0.9 ± 0.7	0.2 ± 0.3	0.08 ± 0.05	100.2
26	Pyrox	9	60.0 ± 0.2	0.3 ± 0.1	0.4 ± 0.1	0.9 ± 0.5	0.12 ± 0.03	39.5 ± 0.4	0.3 ± 0.1	b.d.	0.05 ± 0.03	101.5
37	Pyrox	7	59.4 ± 0.4	0.3 ± 0.1	0.18 ± 0.05	0.5 ±0.2	0.17 ± 0.05	39.4 ± 0.2	0.3 ± 0.1	b.d.	b.d.	100.5
53	Pyrox	8	59.6 ± 0.5	0.3 ± 0.1	b.d	0.4 ± 0.2	b.d	40.0 ± 0.3	0.3 ± 0.2	b.d.	b.d.	100.7
57	Pyrox	4	60 ± 1	0.13 ± 0.06	b.d	1 ± 1	b.d	40.1 ± 0.8	0.2 ± 0.1	b.d.	b.d.	101.3
26	Oliv	1	43.2	b.d.	0.11	0.49	0.14	57.2	0.14	b.d.	b.d.	101.3
3r	Meso.	2	65.4 ± 0.7	21.0 ± 0.2	0.12 ± 0.08	0.1 ± 0.1	b.d.	0.06 ± 0.02	1.5 ± 0.4	7 ± 1	0.27 ± 0.03	96.9
3p	Meso.	22	69 ± 5	20.8 ± 0.6	0.09 ± 0.07	0.13 ± 0.05	b.d.	0.6 ± 0.9	1.1 ± 0.3	0.8 ± 0.3	1.30 ± 0.09	93.1
12	Meso.	6	61 ± 7	21 ± 2	0.1 ± 0.1	0.7 ± 0.9	b.d.	2 ± 3	10 ± 3	4.1 ± 0.8	0.16 ± 0.09	99.8
Pecora Escarpment 91020: EL3												
1	Pyrox	8	61 ± 3	1 ± 1	0.2 ± 0.1	0.6 ± 0.3	0.06 ± 0.03	35 ± 3	0.9 ± 0.9	0.08 ± 0.05	0.08 ±0.06	99.9
4	Pyrox	2	59.6 ± 0.1	0.19 ± 0.02	0.56 ± 0.03	1.08 ± 0.06	0.13 ± 0.02	38.9 ± 0.03	b.d.	b.d.	b.d.	100.5
17	Pyrox	5	59.9 ± 0.3	0.4 ± 0.2	0.2 ± 0.2	0.4 ± 0.3	b.d.	39.6 ± 0.6	0.5 ± 0.2	0.07 ± 0.08	b.d.	101.1
19	Pyrox	3	60 ± 1	0.37 ± 0.01	0.35 ± 0.01	0.57 ± 0.05	0.17 ± 0.01	39.2 ± 0.7	0.4 ± 0.3	b.d.	0.08 ± 0.01	100.6
23	Pyrox	2	59.3 ± 0.6	0.16 ± 0.05	0.2 ± 0.1	1.1 ± 0.4	0.05 ± 0.01	38.6 ± 0.4	0.6 ± 0.6	b.d.	b.d.	100.1
31	Pyrox	1	59.2	0.68	b.d.	0.7	b.d.	39.0	0.5	b.d.	0.05	100.2
41	Pyrox	4	59.7 ± 0.2	0.48 ± 0.1	0.34 ± 0.01	0.5 ± 0.1	0.19 ± 0.08	39.7 ± 0.2	0.3 ± 0.1	b.d.	0.09 ± 0.03	101.3
42	Pyrox	5	60.3 ± 0.1	0.24 ± 0.04	0.1 ± 0.2	0.27 ± 0.09	0.08 ± 0.08	40.1 ± 0.2	0.25 ± 0.08	b.d.	0.05 ± 0.08	101.4
53	Pyrox	4	59.6 ± 0.4	0.11 ± 0.02	b.d.	1.0 ± 0.4	0.12 ± 0.07	39.5 ± 0.2	0.7 ± 0.4	0.05 ± 0.02	b.d.	101.3
57	Pyrox	16	59.5 ± 0.9	0.6 ± 0.5	0.3 ± 0.1	1.1 ± 0.5	0.11 ± 0.07	38 ± 1	0.5 ± 0.4	b.d.	b.d.	100.8
Ul	Pyrox	34	60 ± 1	0.4 ± 0.3	0.40 ± 0.08	1.3 ± 0.4	0.08 ± 0.03	39 ± 1	0.5 ± 0.6	b.d.	0.05 ± 0.02	100.8
4	Oliv.	1	42.9	b.d	0.26	0.51	0.06	57.3	0.09	b.d.	b.d.	101.2
19	Oliv.	1	42.9	0.04	0.11	0.14	0.15	57.6	0.24	b.d.	b.d.	101.2
4	Meso.	2	76 ± 9	16 ± 6	0.15 ± 0.01	0.16 ± 0.02	b.d.	0.6 ± 0.2	0.6 ± 0.6	0.98 ± 0.09	0.18 ± 0.07	96.6
19	Meso.	2	60 ± 1	22 ± 1	0.05 ± 0.02	1.1 ± 0.2	b.d.	9 ± 1	2.1 ± 0.1	0.25 ± 0.05	0.42 ± 0.06	95.7
19r	Meso.	6	63 ± 3	22 ± 1	0.05 ± 0.03	0.9 ± 0.2	b.d.	4 ± 4	1.6 ± 1	1.6 ± 0.5	0.3 ± 0.2	95.9
23	Meso.	4	73 ± 1	20.7 ± 0.9		0.09 ± 0.09	b.d.	0.18 ± 0.02	0.9 ± 0.1	0.11 ± 0.02	b.d.	95.2
41	Meso.	2	62 ± 1	23.9 ± 0.7	0.09 ± 0.01	0.15 ± 0.05	0.13 ± 0.02	6 ± 2	5.1 ± 0.9	0.26 ± 0.02	0.3 ± 0.2	98.7
42	Meso.	10	63 ± 6	25 ± 4		0.15 ± 0.07	b.d.	2 ± 1	4 ± 2	0.3 ± 0.1	b.d.	95.1

TABLE 3. *Continued.*

#	Phase	Pts.	SiO_2	Al_2O_3	Cr_2O_3	FeO	MnO	MgO	CaO	Na_2O	TiO_2	Total*
Pecora Escarpment 91020: EL3 *Continued*												
UI	Meso.	3	65 ± 8	22 ± 2	0.05 ± 0.05	0.11 ± 0.06	b.d.	3 ± 3	4 ± 5	1.1 ± 0.6	0.2 ± 0.2	97.1
Allan Hills 84170: EH3												
2	Pyrox	3	59 ± 1	0.3 ± 0.3	0.3 ± 0.3	0.7 ± 0.2	0.13 ± 0.04	40 ± 1	0.2 ± 0.2	0.06 ± 0.02	b.d.	101.1
13	Pyrox	7	58.8 ± 0.6	0.9 ± 0.8	0.38 ± 0.08	0.6 ± 0.2	0.09 ± 0.02	38.1 ± 0.7	0.5 ± 0.2	b.d.	0.10 ± 0.08	99.7
1	Oliv.	5	42 ± 2	1 ± 2	0.2 ± 0.1	1 ± 1	0.06 ± 0.01	56 ± 2	0.1 ± 0.2	b.d.	b.d.	100.4
11	Oliv.	1	42.7	b.d.	0.33	0.4	0.12	56.4	0.46	b.d.	b.d.	100.5
13	Oliv.	4	42.6 ± 0.6	0.2 ± 0.2	0.3 ± 0.2	0.39 ± 0.03	0.10 ± 0.03	55 ± 1	1 ± 1	b.d.	b.d.	100.7
Pecora Escarpment 91238: EH3												
1	Pyrox	12	59.9 ± 0.9	1 ± 1	0.2 ± 0.1	0.5 ± 0.2	0.06 ± 0.05	38 ± 2	0.11 ± 0.09	0.3 ± 0.5	b.d.	100.4
2	Pyrox	10	59.9 ± 0.2	0.3 ± 0.2	b.d.	0.2 ± 0.1	0.09 ± 0.07	39.7 ± 0.7	0.2 ± 0.2	b.d.	b.d.	100.5
4	Pyrox	13	59 ± 1	0.2 ± 0.2	0.2 ± 0.3	1 ± 1	b.d.	39.2 ± 0.9	0.1 ± 0.1	0.1 ± 0.1	b.d.	100.6
5	Pyrox	6	59.6 ± 0.1	0.4 ± 0.2	0.2 ± 0.2	0.3 ± 0.2	0.1 ± 0.1	39.4 ± 0.3	0.1 ± 0.1	b.d.	b.d.	100.4
2	Oliv.	4	44 ± 1	0.04 ± 0.03	b.d.	0.2 ± 0.3	b.d.	56 ± 1	0.1 ± 0.2	b.d.	b.d.	100.3
5	Oliv.	1	42.8	0.05	b.d.	0.04	b.d.	56.9	b.d.	b.d.	b.d.	100.0
1	Meso.	1	65.5	20.6	b.d.	0.08	b.d.	1.5	0.24	9.25	b.d.	98.2
4	Meso.	2	68 ± 2	18.4 ± 0.1	b.d.	0.6 ± 0.3	b.d.	3 ± 1	0.15 ± 0.06	9.4 ± 0.6	b.d.	100.6
5	Meso.	4	65 ± 2	19 ± 1	0.1 ± 0.1	0.8 ± 0.9	b.d.	4 ± 3	0.19 ± 0.09	9.3 ± 0.9	b.d.	100.5

Abbreviations: Pts. = number of points in average; b.d. = below detection limits; pyrox = pyroxene; Oliv. = olivine; Meso. = mesostasis.
*Includes minor amounts of K_2O and SO_2.

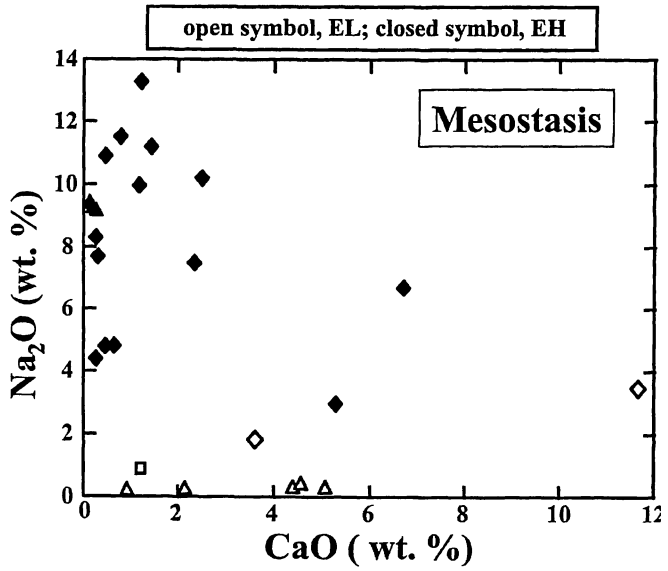

FIG. 8. Na_2O *vs.* CaO for the mesostasis of chondrules in enstatite chondrites. For EL chondrites (open symbols), squares indicate ALH 85119, diamonds indicate MAC 88180, and triangles indicate PCA 91020; for EH chondrites, triangles indicate PCA 91238 (this work) and diamonds indicate Qingzhen (Grossman *et al.*, 1985). The sodium content of EH chondrules is considerably higher than that of EL chondrules, rarely falling below 4 wt%. This high concentration of sodium in the mesostasis of chondrules from EH3 chondrites may be reflecting differences in precursor materials or, more likely, is due to differences in accretionary processes occurring in the enstatite chondrites.

DISCUSSION

Comparison of Chondrules from EH and EL Chondrites

Chondrules in EL and EH chondrites are very similar with respect to their range and distribution of textures, major CL properties, and the composition of silicates (Tables 1 and 3; Figs. 1 and 7). An exception is that barred-Ol-Px chondrules, observed in the EH3 chondrite Y-691 by Ikeda (1989), have not been observed among our EL chondrules. The similarities in the range and distribution of textures would indicate that the chondrules of both meteorite types have undergone similar cooling rates and nucleation histories, while the similarities in CL color and silicate compositions indicate similar precursor materials.

The difference in CL properties, namely the bright red CL of the enstatite in the EL chondrules, is due to the presence of "dusty" metal in the pyroxene (Fig. 6). Chondrules from both EH and EL chondrites contain this dusty material, but it occurs in most enstatite grains in EL chondrules, and is thus more readily apparent in the CL of the silicates. The appearance of small globules of Fe-metal and troilite in silicates in the EH3 chondrite Y-691 was reported by Ikeda (1989), where it was attributed to liquid immiscibility between silicate and metal–sulfide melts. Alternatively, dusty metal has been reported in olivine of ordinary chondrites, where it was attributed to *in situ*

TABLE 4. Bulk composition (wt%) of chondrules in EL3 and EH3 chondrites.

#	Pts.	SiO_2	Al_2O_3	Cr_2O_3	FeO	MnO	MgO	CaO	Na_2O	TiO_2	Total*
MacAlpine Hills 88180: EL3											
3	25	59 ± 3	6 ± 6	0.3 ± 0.1	2 ± 2	0.10 ± 0.04	29 ± 11	1 ± 1	2 ± 3	0.1 ± 0.1	99.9
12	15	56 ± 4	3 ± 3	0.7 ± 0.9	2 ± 2	0.10 ± 0.04	35 ± 8	1 ± 2	0.5 ± 0.6	0.11 ± 0.06	99.7
Allan Hills 85119: EL3											
21	24	54 ± 5	2 ± 3	0.4 ± 0.2	5 ± 6	0.01 ± 0.06	35 ± 4	0.9 ± 0.7	0.4 ± 0.7	0.07 ± 0.05	99.7
37	11	54 ± 5	4 ± 4	0.2 ± 0.2	3 ± 2	0.01 ± 0.05	35 ± 7	0.9 ± 0.7	1 ± 1	0.12 ± 0.06	99.1
Pecora Escarpment 91020: EL3											
41	14	53 ± 7	2 ± 2	0.31 ± 0.07	1.1 ± 0.4	0.20 ± 0.05	42 ± 8	0.8 ± 0.7	0.5 ± 0.8	0.09 ± 0.07	100.5
ul	12	58 ± 3	3 ± 5	0.4 ± 0.1	2 ± 1	0.08 ± 0.04	34 ± 9	0.6 ± 0.4	1 ± 2	0.05 ± 0.02	100.1
19	18	51 ± 6	3 ± 2	0.25 ± 0.06	3 ± 1	0.20 ± 0.06	40 ± 8	2 ± 1	0.7 ± 0.9	0.11 ± 0.09	100.8
Pecora Escarpment 91238: EH3											
1	29	57 ± 2	4 ± 2	0.3 ± 0.1	2 ± 2	0.08 ± 0.03	33 ± 5	0.3 ± 0.2	1 ± 1	b.d.	100.4
2	25	58 ± 2	2 ± 2	0.09 ± 0.07	1 ± 1	0.12 ± 0.06	38 ± 5	0.4 ± 0.4	1 ± 1	0.05 ± 0.04	100.5
4	47	58 ± 5	0.7 ± 0.9	0.2 ± 0.3	3 ± 3	0.05 ± 0.05	37 ± 8	0.2 ± 0.2	0.3 ± 0.4	b.d.	100.3
5	17	60 ± 1	4 ± 4	0.2 ± 0.1	0.7 ± 0.4	0.15 ± 0.08	33 ± 8	0.3 ± 0.2	2 ± 2	0.06 ± 0.05	100.5

Abbreviations: Pts. = number of points in average; b.d. = below detection limits.
*Includes minor amounts of K_2O and SO_2.

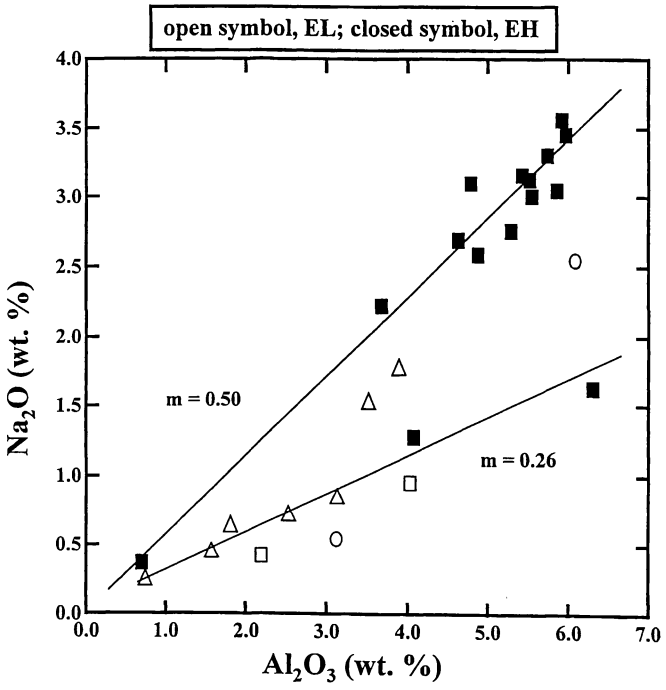

FIG. 9. Bulk Na and Al compositions of chondrules from EH and EL chondrites. For EL chondrites (open symbols), squares indicate ALH 85119, circles indicate MAC 88180, and triangles indicate PCA 91020; for EH chondrites, triangles indicate PCA 91238 (this work) and squares indicate Qingzhen (Grossman *et al.*, 1985). The bulk Na_2O/Al_2O_3 composition of EH chondrules is greater than that of EL chondrules by about a factor of 2, reflected by a higher slope on the best-fit line. This suggests that the difference in mesostasis composition (see Fig. 8) is not simply due to diffusion of the sodium out of the mesostasis into the silicates in chondrules from EL3 chondrites. The relatively small amounts of Na_2O and Al_2O_3 are a reflection of the small amounts of mesostasis present in these chondrules.

reduction of FeO from the host olivine (Rambaldi and Wasson, 1982). The mechanism by which the metal affects the CL color is not clear: conductive materials do not typically exhibit CL (*e.g.*, Marshall, 1988).

The difference in sizes of the chondrules in the two classes, and within each class, also gives important insights into the formation of these objects. Rubin and Grossman (1987) attributed the fact that nonporphyritic chondrules in EH chondrites predominate the smaller sizes to preferential disruption of large nonporphyritic droplets during formation. The domination of nonporphyritic chondrules in the larger size fraction, which Rubin and Grossman found difficult to explain, was not observed in our data, although we are dealing with a smaller number of chondrules. The even distribution of sizes in both textural types of the EL chondrites would seem to indicate that the disruptive event occurring during the formation of nonporphyritic chondrules did not take place in the EL chondrites.

Another major difference in the chondrules, the Na content in the mesostasis, is an important indicator of a divergence in events somewhere in the history of these two chondrite types. This idea will be explored in more detail below.

Classification of Enstatite Chondrite Chondrules

One of the goals of this study was to examine the value of a classification system for the chondrules in enstatite chondrites similar to that created by Sears *et al.* (1992) for ordinary chondrite chondrules. Based on our data, it is clear that a scheme for the chondrules of ordinary chondrites will not simply apply to highly reduced chondrules such as those in enstatite chondrites. One criteria used by Sears *et al.* (1992) to evaluate

chondrules was mesostasis composition. On a ternary plot of the normative albite, quartz, and anorthite compositions of the mesostasis, the EH3 chondrule mesostases display an albitic composition, while EL3 chondrule mesostasis is primarily quartz normative (Fig. 10). Using this scheme, EH chondrules would be primarily type A5 chondrules, with some B2 and B3, while EL chondrules would be essentially B1 types. However, the olivine and pyroxene compositions are consistent with FeO-poor type A1 and A2 chondrules (Fig. 11a,b). Moreover, the CL characteristics of the chondrules in enstatite chondrites differ from those of chondrules in ordinary chondrites (Sears *et al.*, 1992). Thus the compositional classification scheme for chondrules in ordinary chondrites cannot be applied directly in its current form to the chondrules in enstatite chondrites. The major differences that appear in the chondrules of the two types of enstatite chondrite (CL color, size distribution and mesostasis composition) are already divided by EH and EL subtypes, with the same chondrule textures (PP, POP, RP, G, C) being fairly evenly distributed between the two classes. This indicates that the classification of chondrules in the enstatite chondrites by texture and class will suffice for first-order classifications. The differences seen in the chondrules of the two classes reveal important information about early processes occurring in chondrite formation, as we will discuss below.

Implications for the Origin of the EH and EL Chondrites

The many similarities of the chondrules in EH and EL chondrites suggest similar histories, but their differences in size and Na composition of the mesostasis indicates important differences in the histories of chondrules from the two classes of enstatite chondrite. These differences must be occurring either (1) in the precursor materials, or (2) in the formation of the chondrules and their subsequent accretion, or (3) during parent-body alteration. Here we discuss which of these is most likely.

Precursor Materials–If the chondrules of the two classes of enstatite chondrite were formed from two chemically different sets of precursor materials, this would be expected to show up in various aspects of the chondrules, including O-isotopic compositions. Very few data exist for the O-isotopic

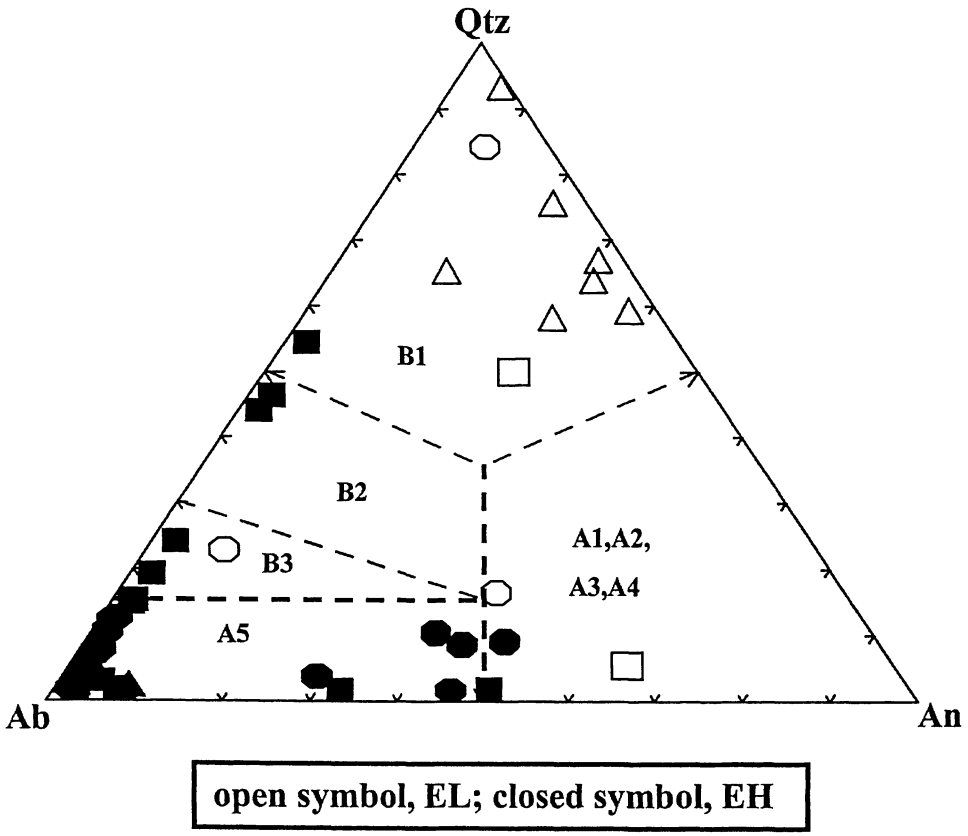

FIG. 10. Normative mesostasis composition of EH and EL chondrules on a quartz–anorthite–albite ternary. Each data point represents an individual chondrule. For EL chondrites (open symbols), squares indicate ALH 85119, circles indicate MAC 88180, and triangles indicate PCA 91020; for EH chondrites (filled symbols), triangles indicate PCA 91238 (this work), squares indicate Qingzhen (Grossman *et al.*, 1985) and circles indicate Y-691 (Ikeda, 1989). Dashed lines indicate the fields for chondrules of ordinary chondrites on the same ternary (after Sears *et al.*, 1992). By these criteria, chondrules in EL chondrites would be essentially type B1, while chondrules in EH chondrites would be largely type A5.

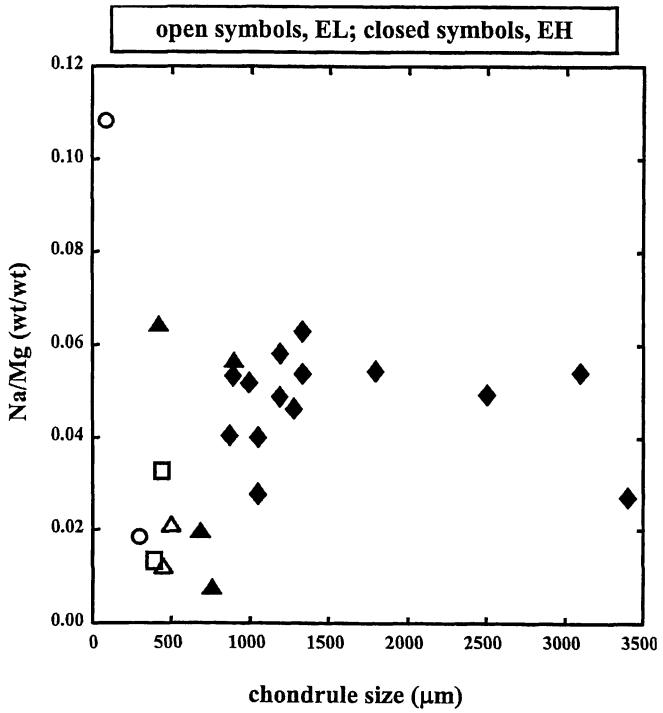

FIG. 11. Sodium/magnesium values *vs.* diameter for chondrules in EH and EL chondrites. For EL chondrites (open symbols), squares indicate ALH 85119, circles indicate MAC 88180, and triangles indicate PCA 91020; for EH chondrites (filled symbols), triangles indicate PCA 91238 (this work), and diamonds indicate Qingzhen (Grossman *et al.*, 1985). A positive correlation between size and composition indicates that the low sodium content of most chondrules in EL chondrites may be due to evaporative loss of Na from these objects.

compositions of chondrules in EH chondrites (Clayton and Mayeda, 1985), and none for those in EL chondrites. However, the whole-rock O-isotopic compositions of unequilibrated enstatite chondrites lie along the terrestrial fractionation line of slope 0.5, while the EH chondrites line along another line of slope 0.66 (Clayton and Mayeda, 1985; Newton *et al.*, 2000). If whole-rock O-isotopic compositions mirror chondrule compositions, then the O isotopes may indicate differences in the two classes, but whether this is due to nebular processes creating different precursors or to subsequent parent-body processes is unclear.

Differences in precursors might also be expected to affect subsequent chondrule sizes and mesostasis compositions during chondrule formation. For example, one factor that could relate the size and composition of the chondrules is that of viscosity. If the bulk compositions of one class caused the melt to be more viscous than another, we would predict larger droplets (*e.g.*, Lundgren and Mansour, 1988; Wang *et al.*, 1994), and thus larger chondrules. Figure 12 shows data for the viscosity of the diopside–albite–anorthite system, which approximates the composition of enstatite chondrules (Kozu and Kani, 1934). For any given temperature, the viscosity of the mixture generally increases with an increased Na_2O composition. A similar formation temperature can be assumed for both EH and EL chondrules, based on the high-temperature mineral thermometers (Zhang and Sears, 1996), so both classes may be compared in terms of the relationship between viscosity and volatile content; therefore chondrules with a higher Na content would be expected to be larger. Figure 13 shows the bulk chondrule Na/Mg abundance as a function of chondrule size for the chondrules studied here, as well as for chondrules in Qingzhen (Grossman *et al.*, 1985). The relationship between chondrule size and Na abundance indicates the EL chondrules, with lower abundances of Na, are generally smaller than Na-rich chondrules from EH chondrites The larger chondrules contain an increasingly higher abundance of Na, up to a Na/Mg ratio of ~0.06. This might indicate a relationship between the Na content of the melt and its viscosity, which potentially might mean the Na difference might arise from chemically different precursors. However, due to evidence from oxygen isotopes and chemical fractionation that indicate chondrules may have undergone multiple melting episodes (*e.g.*, Hewins, 1996) and are "recycled", it is difficult to believe that the chondrules' current compositions reflect the original precursor materials.

It must be noted that the chondrules in the EH chondrites used for bulk studies in this work were chosen for their relatively large mesostasis content (which was generally low to nonexistent) which effectively caused the selection of larger chondrules for study. Also, the sizes of chondrules in this work were measured in thin section, while the sizes of chondrules from the literature data in Fig. 13 are for chondrules physically separated from the bulk rock, and thus representing the largest chondrules in the meteorite. An alternative interpretation, mentioned below, is that the sodium content of the mesostatis reflects post-accretionary transport into the mesostasis rather than accretionary origin.

Chondrule Formation/Accretion–If the chondrules of the two classes of enstatite chondrites formed from the same precursors, and the difference in the Na content came about due to divergent events during the formation of the chondrules and/or their subsequent accretion into the whole rock, then we must address the problem of whether Na is being enriched in the EH chondrules or depleted in the EL chondrules. If the chondrules acted as an open system during formation (Huang *et al.*, 1996), then the problem becomes that of maintaining the volatile Na in the chondrules. One possibility is that the chondrules of EH chondrites formed in a high-Na vapor environment. Lewis *et al.* (1993) showed that the Na content of chondrules could be maintained and even enriched under a high-temperature and chondritic fO_2 environment by keeping the chondrules in a Na-rich vapor. Thus the mesostasis difference between the EH and EL chondrules could mean that while formation conditions were similar, the EH chondrules formed in a region of higher Na vapor content. The creation or stability of such a high Na vapor pressure is not well constrained,

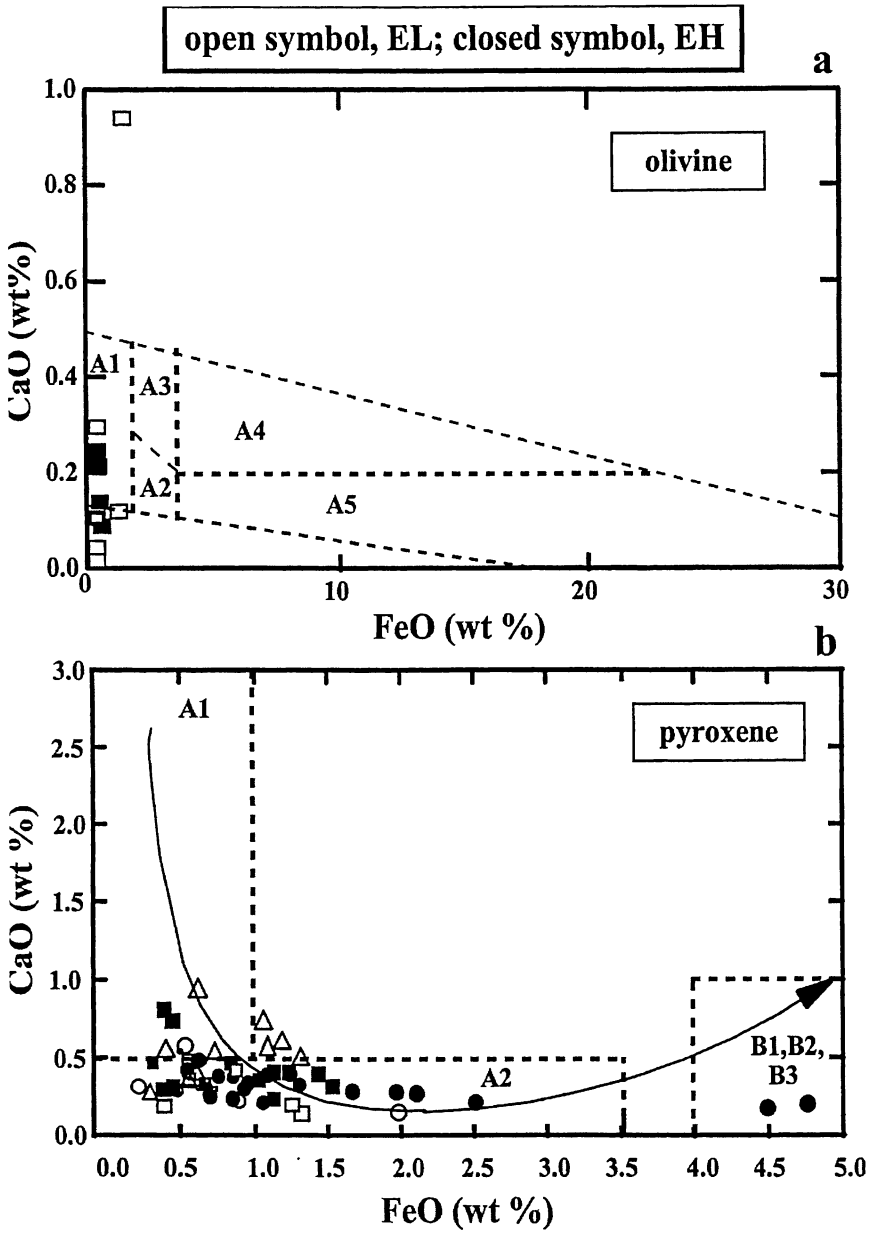

FIG. 12. (a) CaO *vs.* FeO in olivines of EH and EL chondrules. The superimposed fields are for chondrules in ordinary chondrites, as established by Sears *et al.* (1995). According to this scheme, all enstatite chondrite chondrules fall in the A1 field or below the range of the ordinary chondrules, with no separation between the EH and EL chondrule olivines. (b) CaO *vs.* FeO in pyroxenes in enstatite chondrite chondrules. For EL chondrites (open symbols), squares indicate ALH 85119, circles indicate MAC 88180, and triangles indicate PCA 91020; for EH chondrites, circles indicate Y-691 (Ikeda, 1989) and squares indicate Qingzhen (Grossman *et al.*, 1985). Field lines are those for ordinary chondrite chondrules from Sears *et al.* (1995). If this scheme was applied to the enstatite chondrites, all chondrules in enstatite chondrites would be type A1–A2, again with no apparent distinction between EH and EL.

but has been suggested as a setting for at least one group of chondrules found in the ordinary chondrites (Matsunami *et al.*, 1993). Due to the very limited amount of mesostasis in chondrules in estatite chondrites, however, it is not possible to test this idea by searching for changes in Na content as a function of distance from the chondrule edge, unlike the ordinary chondrites. Alternatively, the chondrules of both EH and EL chondrites may have formed with relatively high amounts of sodium, and the Na in chondrules of EL chondrites was subsequently mobilized out of the chondrules, an idea that we shall discuss in the next section.

The size difference of the chondrules in EH and EL chondrites may also have occurred during their formation or subsequent accretion. If the size distribution is a primary effect

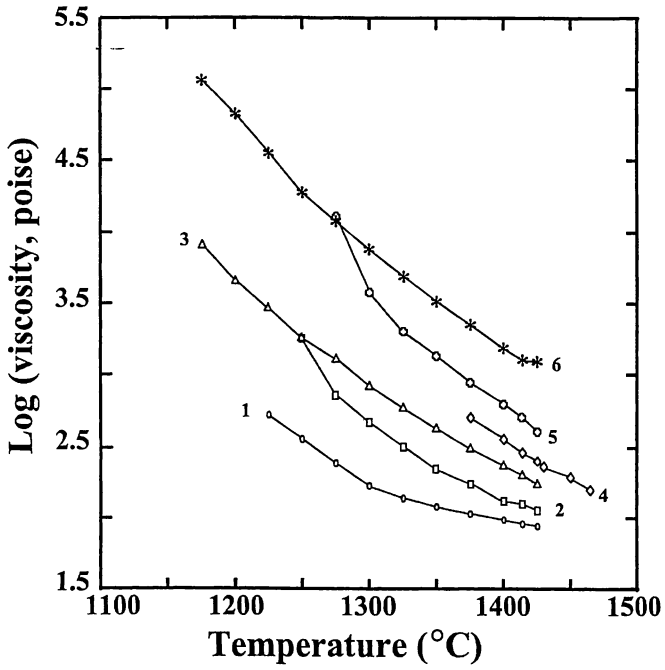

FIG 13. Viscosity–temperature data for the diopside–albite–anorthite system (from Kozu and Kani, 1934). This system is an approximation to the composition of chondrules in enstatite chondrites. The numbers near each data set indicate the percent by mass of diopside-albite-anorthite (1 = 60-20-20 , 2 = 40-40-20, 3 = 40-20-40, 4 = 20-60-20, 5 = 20-40-40, 6 = 20-20-60). The viscosity generally increases as the amount of the sodium-bearing mineral albite increases.

of the formation of the chondrules, it may be due to ballistic sorting of the chondrules, or it may have occurred after chondrule formation and prior to accretion (*e.g.*, Whipple, 1972), such as through the size sorting of particles in a dynamic regolith as described by Akridge and Sears (1999). A steady flow of volatiles moving through the regolith could have produced conditions resembling a fluidized bed in which density and size sorting of materials occur. Envisioning such a scenario for the enstatite chondrites, the larger EL chondrules would remain buried in the regolith and the bulk rock would cool slowly over time, while the smaller EH chondrules would be carried upward by degassing events in the regolith, where insulating effects would be lesser and thus the bulk EH material would experience more rapid cooling. Thus, the scenario we imagine is one in which the EH and EL chondrules formed in similar environments using similar precursors and were subsequently size sorted and rapidly incorporated into the bulk rock. Following accretion of the whole rock, the EH chondrites underwent rapid cooling and thus retained their Na while the more slowly-cooled EL chondrites lost Na through volatilization and diffusion. Sulfide chemistry has been used to argue for cooling rates of 6 °C/h for EL chondrites, compared with 10^3–10^4 °C/h for EH chondrites (Zhang and Sears, 1996; Zhang *et al.*, 1996). This large difference in cooling rates would support a scenario as described above.

Parent-Body Alteration–Subsequent processing of the chondrite parent body after accretion may account for some of the observed properties of the chondrules. The sodium content of EL chondrule mesostasis possibly reflects mobilization of sodium during metamophism. Evidence from Rb-Sr, K-Ar, and Ar-Ar studies indicate that unequilibrated EH chondrites underwent a late thermal event around 1.5–3 Ga ago (Honda *et al.*, 1982; Shima *et al.*, 1983; Jessberger, 1983; Torigoye and Shima, 1993), consistent with reheating of the parent body at a low (possibly 500 °C) temperature (Torigoye and Shima, 1993). In looking at more metamorphosed enstatite chondrites, the difference in major element abundances (*e.g.*, bulk Fe/Si, Mg/Si, S/Si, Si in kamacite) observed between the EH and EL chondrites is echoed by a hiatus in iodine isotopic composition as well, and it is presumed that the same process is being reflected for both differences (Kennedy *et al.*, 1988). Interpretations of this include the possibility that the iodine isotopic compositions are reflecting a real age difference, or the possibility they reflect nebular isotopic heterogeneity. According to Kennedy *et al.*, if the iodine isotopic compositions are reflecting real age differences in meteorites which originated from a common reservoir, this could be dating the agglomeration of metal and silicate. In this case, the difference in both chemical compositions and I-Xe ages would be consistent with the model of Baedecker and Wasson (1975) in which agglomeration of the metal-rich EH chondrites would precede that of the silicate-rich EL chondrites.

CONCLUSIONS

To summarize this study, the chondrules of EH and EL chondrites are similar in most respects, including textural distributions, major CL properties, and silicate compositions, but differ in some important respects (*i.e.*, their size distributions (with EH > EL), minor CL properties and Na composition of the mesostasis). From these observations we make several inferences. First, we do not observe enough significant differences in chondrules within a given class to allow for a unique subclassification of the chondrules as with chondrules in ordinary chondrites, and propose that the current classifications by textural types between EH and EL are sufficient. Second, the differences we observe between chondrules of the two classes, particularly the mesostasis difference, do not seem to indicate different precursors for the two types of chondrules. Instead we feel that the chemical fractionation and size differences of the chondrules are reflecting their creation from similar precursors in similar environments and by similar processes, followed by subsequent size sorting and rapid incorporation into the bulk rock; following accretion of the whole rock, the EH chondrites underwent rapid cooling while the EL chondrites cooled more slowly.

Acknowledgments–We wish to thank Alan Rubin, Alex Ruzicka, and Ed Scott for their comments and suggestions in improving this

manuscript. We also wish to thank Gordon McKay for access to the Johnson Space Center electron microprobe facility, and Yanhong Zhang, Glen Akridge, and Jannette Akridge for their help and support.

Editorial handling: E. R. D. Scott

REFERENCES

AKRIDGE D. G. AND SEARS D. W. G. (1999) The gravitational and aerodynamic sorting of meteoritic chondrules and metal: Experimental results with implications for chondritic meteorites. *J. Geophys. Res.* **104**, 11 853–11 864.

BAEDECKER P. A. AND WASSON J. T. (1975) Elemental fractionations among enstatite chondrites. *Geochim. Cosmochim. Acta* **39**, 735–765.

CLAYTON R. N. AND MAYEDA T. K. (1985) Oxygen isotopes in chondrules from enstatite chondrites: Possible identification of a major nebular reservoir (abstract). *Lunar Planet Sci.* **16**, 142–143.

DEHART J. M., LOFGREN G. E., LU J., BENOIT P. H. AND SEARS D. W. G. (1992) Chemical and physical studies of chondrites X: Cathodoluminescence studies of metamorphism and nebular processes in type 3 ordinary chondrites. *Geochim. Cosmochim. Acta* **56**, 3791–3807.

DODD R. T. (1981) *Meteorites: A Petrologic–Chemical Synthesis*. Cambridge Univ. Press, New York, New York, USA. 368 pp.

EISENHOUR D. D. (1996) Determining chondrule size distributions from thin-section measurements. *Meteorit. Planet. Sci.* **31**, 243–248.

GOODING J. L. AND KEIL K. (1981) Relative abundances of chondrule primary textural types in ordinary chondrites and their bearing on conditions of chondrule formation. *Meteoritics* **16**, 17–43.

GROSSMAN J. N. AND SCORE R. (1996) The Meteoritical Bulletin, No. 79, 1996 July: Recently classified specimens in the United States Antarctic Meteorite Collection (1994–1996). *Meteorit. Planet. Sci.* **31 (Suppl.)**, A161–A174.

GROSSMAN J. N., RUBIN A. E., RAMBALDI E. R., RAJAN R. S. AND WASSON J. T. (1985) Chondrules in the Qingzhen type-3 enstatite chondrite: Possible precursor components and comparison to ordinary chondrite chondrules. *Geochim. Cosmochim. Acta* **49**, 1781–1795.

HEWINS R. H. (1996) Chondrules and the protoplanetary disk: An overview. In *Chondrules and the Protoplanetary Disk* (eds. R. H. Hewins, R. H. Jones and E. R. D. Scott), pp. 3–9. Cambridge University Press, New York, New York, USA.

HONDA M., BERNATOCWICZ T. J. AND PODOSEK F. A. (1982) ^{129}Xe-^{128}Xe and ^{40}Ar-^{39}Ar chronology of two Antarctic enstatite meteorites. *Mem. Natl. Inst. Polar Res., Spec. Issue* **30**, 275–291.

HUANG S., LU J., PRINZ M., WEISBERG M. K., BENOIT P. H. AND SEARS D. W. G. (1996) Chondrules: Their diversity and the role of open-system processes during their formation. *Icarus* **122**, 316–346.

IKEDA Y. (1988) Petrochemical study of the Yamato-691 enstatite chondrite (E3) I: Major element chemical compositions of chondrules and inclusions. *Proc. NIPR Symp. Antarct. Meteorites* **1**, 3–13.

IKEDA Y. (1989) Petrochemical study of the Yamato-691 enstatite chondrite (E3) III: Descriptions and mineral compositions of chondrules. *Proc. NIPR Symp. Antarct. Meteorites* **2**, 75–108.

JESSBERGER E. K. (1983) Ar-Ar ages of carbonaceous and enstatite chondrites (abstract). *Meteoritics* **18**, 321.

JONES R. H. (1990) Petrology and mineralogy of type II, Fe-rich chondrules in Semarkona (LL3.0): Origin by closed-system fractional crystallization, with evidence for supercooling. *Geochim. Cosmochim. Acta* **54**, 1785–1802.

JONES R. H. (1994) Petrology of FeO-poor, porphyritic pyroxene chondrules in the Semarkona chondrite. *Geochim. Cosmochim. Acta* **58**, 5325–5340.

KENNEDY B. M., HUDSON B., HOHENBERG C. M. AND PODOSEK F. A. (1988) $^{129}I/^{127}I$ variations among enstatite chondrites. *Geochim. Cosmochim. Acta* **52**, 101–111.

KING T. V .V. AND KING E. A. (1978) Grain size and petrography of C2 and C3 carbonaceous chondrites. *Meteoritics* **13**, 47–72.

KING T. V. V. AND KING E. A. (1979) Size frequency distributions of fluid drop chondrules in ordinary chondrites. *Meteoritics* **14**, 91–96.

KOZU S. AND KANI K. (1934) Viscosity measurement of the ternary system diopside–albite–anorthite at high temperatures. *Imp. Acad. Japanese Proc.* **10**, 29–32.

LEITCH C. A. AND SMITH J. V. (1982) Petrography, mineral chemistry and origin of type I enstatite chondrites. *Geochim. Cosmochim. Acta* **46**, 2083–2097.

LEITCH C. A., SMITH J. V., SMITH M. R. AND SCHMITT R. A. (1982) Microscopic properties and bulk chemistry of individual chondrules of the Indarch enstatite chondrite (abstract). *Meteoritics* **17**, 243–244.

LEVIN E. M., ROBBINS C. R. AND MCMUNDIE A. F. (1964) *Phase Diagrams for Ceramists*. American Ceramic Society, Waterville, New York, USA. 2066 pp.

LEWIS R. D., LOFGREN G. E., FRANZEN H. F. AND WINDOM K. E. (1993) The effect of Na vapor on the Na content of chondrules. *Meteoritics* **28**, 622–628.

LUNDGREN T. S. AND MANSOUR N. N. (1988) Oscillations of drops in zero gravity with weak viscous effects. *J. Fluid Mech.* **194**, 479–510.

MARSHALL D. J. (1988) *Cathodoluminescence of Geological Materials*. Unwin Hyman, London, U.K. 146 pp.

MATSUNAMI S. *ET AL.* (1993) Thermoluminescence and compositional zoning in the mesostasis of a Semarkona group A1 chondrule and insights into the chondrule-forming process. *Geochim. Cosmochim. Acta* **57**, 2101–2110.

MCSWEEN H. Y. (1977a) Chemical and petrographic constraints on the origin of chondrules and inclusions in carbonaceous chondrites. *Geochim. Cosmochim. Acta* **41**, 1843–1860.

MCSWEEN H. Y. (1977b) Carbonaceous chondrites of the Ornans type: A metamorphic sequence. *Geochim. Cosmochim. Acta* **41**, 477–491.

NAKAMURA T., TOMEOKA K. AND TAKEDA H. (1992) Shock effects of the Leoville CV carbonaceous chondrite: A transmission electron microprobe study. *Earth Planet. Sci. Lett.* **114**, 159–170.

NAKAMURA T., TOMEOKA K., SEKINE T. AND TAKEDA H. (1995) Impact-induced chondrule flattening in the Allende CV3 carbonaceous chondrite: Shock experiments. *Meteoritics* **30**, 344–347.

NEWTON J., FRANCHI I. A. AND PILLINGER C. T. (2000) The oxygen-isotopic record in enstatite meteorites. *Meteorit. Planet. Sci.* **35**, 689–698.

RAMBALDI E. R. AND WASSON J. T. (1982) Fine, nickel-poor Fe-Ni grains in the olivine of unequilibrated ordinary chondrites. *Geochim. Cosmochim. Acta* **46**, 929.

RAMBALDI E. R., RAJAN R. S., WANG D. AND HOUSLEY R. M. (1983) Evidence for relic grains in chondrules of Qingzhen, an E3 type enstatite chondrite. *Earth Planet. Sci. Lett.* **66**, 11–24.

RUBIN A E. (1989) Size-frequency distributions of chondrules in CO3 chondrites. *Meteoritics* **24**, 179–189.

RUBIN A .E. AND KEIL K. (1984) Size-distributions of chondrule types in the Inman and Allan Hills A77011 L3 chondrites. *Meteoritics* **19**, 135–143.

RUBIN A. E. AND GROSSMAN J. N. (1987) Size-frequency-distributions of EH3 chondrules. *Meteoritics* **22**, 237–251.

RUBIN A. E., SCOTT E. R .D. AND KEIL K. (1997) Shock metamorphism of enstatite chondrites. *Geochim. Cosmochim. Acta* **61**, 847–858.

SCOTT E. R. D. AND TAYLOR G. J. (1983) Chondrules and other components in C, O, and E chondrites: Similarities in their

properties and origins. *Proc. Lunar Planet. Sci. Conf.* **14th**, *J. Geophys. Res.* **88**, B275–B286.

SCOTT E. R. D., KEIL K. AND STÖFFLER D. (1992) Shock metamorphism of carbonaceous chondrites. *Geochim. Cosmochim. Acta* **46**, 597–608.

SEARS D. W. G., LU J., BENOIT P. H., DEHART J. M. AND LOFGREN G. E. (1992) A compositional classification scheme for meteoritic chondrules. *Nature* **357**, 207–210.

SEARS D. W. G., HUANG S. AND BENOIT P. H. (1995) The formation of chondrules (abstract). *Lunar Planet. Sci.* **26**, 1263–1264.

SHIMA M., WAKABAYASHI F., TAKAOKA N. AND OKADA A. (1983) Qingzhen enstatite chondrite (abstract). *Meteoritics* **18**, 395–396.

SMITH J. V., SMITH M. R. AND SCHMITT R. A. (1983) Chemical composition of 24 chondrules in Indarch E4 chondrite (abstract). *Lunar Planet. Sci.* **14**, 714–715.

TORIGOYE N. AND SHIMA M. (1993) Evidence for a late thermal event of unequilibrated enstatite chondrites: A Rb-Sr study of Qingzhen and Yamato 6901 (EH3) and Khairpur (EL6). *Meteoritics* **28**, 515–527.

WANG T. G., ANILKUMAR A. V., LEE C. P. AND LIN K. C. (1994) Bifurcation of rotating liquid drops: Results from USML-1 experiments in space. *J. Fluid Mech.* **276**, 389–403.

WEISBERG M. K., PRINZ M. AND FOGEL R. A. (1994) The evolution of enstatite and chondrules in unequilibrated enstatite chondrites: Evidence from iron-rich pyroxene. *Meteoritics* **29**, 362–373.

WHIPPLE F. L. (1972) On certain aerodynamic processes for asteroids and comets. In *From Plasma to Planet, Nobel Symp.* 21 (ed. A. Elvius), pp. 211–232. John Wiley, New York, New York, USA.

ZHANG Y. AND SEARS D. W. G. (1996) The thermometry of enstatite chondrites: A brief review and update. *Meteorit. Planet. Sci.* **31**, 647–655.

ZHANG Y., HUANG S., SCHNEIDER D., BENOIT P. H., DEHART J. M., LOFGREN G. E. AND SEARS D. W. G. (1996) Pyroxene structures, cathodoluminescence and the thermal history of the enstatite chondrites. *Meteorit. Planet. Sci.* **31**, 87–96.